Evolution of the Alboran Sea hydrographic structures during July 1993

Jesús García Lafuente[a,*], Natalio Cano[b], Manuel Vargas[b], Juan P. Rubín[b], Alonso Hernández-Guerra[c]

[a] *Departamento de Física Aplicada II, Universidad de Málaga, Málaga, Spain*
[b] *Centro Oceanográfico de Málaga, Instituto Español de Oceanografía, Málaga, Spain*
[c] *Departamento de Física, Universidad de Las Palmas de Gran Canaria, Las Palmas, Spain*

Abstract

During the ICTIOALBORAN-0793 multidisciplinary oceanographic survey carried out in July 1993 by the Instituto Español de Oceanografía (IEO) in the Alboran Sea, some anomalous features were detected. One was the presence of a small cyclonic eddy in the western Alboran Basin, close to the African coast. The upper layer of the eddy consisted of Mediterranean Surface Water and was separated from its supposed source (the northern Alboran Sea) by the Atlantic Jet. Another feature was the probable temporary interruption of the flow of fresh Atlantic Water ($S \approx 36.5$) into the eastern Alboran Basin and its replacement by a modified (saltier) Atlantic Water. These features can be explained assuming a time evolution of the surface circulation in the Alboran Sea forced by speed variations in the inflowing Atlantic Water through the Strait of Gibraltar. A collection of satellite images covering the survey period and across-strait sea level difference data, indicative of the geostrophic velocity of the inflow through the Strait, were used to check this assumption. Both sets of data supplied independent but compatible information in the sense that they complemented each other and gave support to the proposed evolving model. Finally, some speculative ideas attempting to correlate the inferred variability in the Alboran Sea with the state of the baroclinic water exchange through the Strait of Gibraltar (maximal or submaximal) are discussed. © 1998 Elsevier Science Ltd. All rights reserved.

1. Introduction

The geographical location of the Alboran Sea as the first Mediterranean basin for the inflowing Atlantic Water (AW) through the Strait of Gibraltar along its path into

---

* Author to whom correspondence should be addressed: Department of Applied Physics II, University of Málaga, Plaza de El Ejido s/n, 29013 Málaga, Spain.

the Mediterranean Sea, makes its study a subject of prime importance for any well-based research on the surface circulation of the Western Mediterranean Sea. During recent decades, not only large international field Experiments (Project Alboran, Lanoix, 1974; Donde Va Group, 1984; Western Mediterranean Circulation Experiment, La Violette, 1990) but also others of a more limited scope (Seco, 1959; Donguy, 1962; Cano, 1977; Parrilla, 1984; Tintore et al., 1991; Rubín et al., 1994) have taken place in this region, aiming at a better understanding of its dynamics.

Despite differences in the results presented in these works, there is a general agreement about the surface circulation pattern: the inflowing AW through the Strait follows a wave-like path toward the east enclosing and feeding two anticyclonic gyres in which AW accumulates. These are known as the western (WG) and eastern gyres (EG), separated by the 3°W meridian, where the prominent Cape Tres Forcas and Alboran Island are situated. While the WG seems to be a rather permanent feature, there is some controversy about the permanency of the EG, which sometimes has not been detected (Lanoix, 1974; Cano, 1977). Numerical (Preller, 1986; Werner et al., 1988; Heburn and La Violette, 1990; Speich, 1992) and laboratory models (Whitehead and Miller, 1979; Gleizon, 1994) show the importance that properties of the inflowing AW through the Strait of Gibraltar and the geometry and topography of the Alboran Basin have on the formation, size, location and energy of the gyres. Though they do not all agree on the basic mechanism generating the gyres, their models reproduce the WG-Jet structure and coupling rather well, but are not so successful in reproducing the EG, which is more elusive. However, Heburn and La Violette (1990), after an intensive analysis of a large set of infrared images extending over a 10-year period, suggest that the presence of the EG is as probable as the apparently more permanent WG, pointing to a significant time variability of the Alboran Sea circulation. The mentioned experimental works do not investigate this variability, since they deal with synoptic data (strictly speaking, quasi-synoptic data). The whole set of *in situ* data available in this region (a large set indeed) is adequate only for statistical studies of the variability and does not permit the evolution of a given situation to be followed. Neither do numerical and laboratory models, since they reproduce a steady situation (after completing a transient state), which is basically determined by the initial and boundary conditions. Data analysed in this work are also of quasi-synoptic type. However, in our opinion, some of the results obtained can be interpreted correctly only if we consider an evolution of the circulation during the 15-day period of the survey.

Certain biological parameters (fish larvae concentration) are most useful to prove this hypothesis. At intermediate depths there are significant horizontal temperature gradients, warmer water being at the southern part of the Alboran Sea because this is preferably occupied by the anticyclonic gyres that accumulate AW. That temperature difference accounts for specific distribution of biological species. Studies of meso-pelagic fish based on its larvae distribution confirm that those of Arctic-boreal nature prevail north of the 36°N parallel (which, roughly, divides the Alboran Basin into two halves, see Fig. 1) while those of temperate–subtropical nature live in the southern half (Rubín et al., 1997). Mesoscale eddies can trap and accumulate biological matter and

produce episodic colonizations of remote habitats when they are advected by the mean current (Lobel and Robinson, 1986; Mullineaux, 1993). Ichthyoplanktonic species of unequivocal taxonomic identification represent valuable biological tracers for water mass motions.

This paper intends to contribute to the knowledge of the surface circulation variability of the Western Alboran Sea, starting from the identification of some dynamic features observed during July 1993. The paper is organized as follows. Section 2 presents the dataset and some consideration of its synopticity. Section 3 describes the features that have made us reflect on an eddy shedding from the Atlantic Jet at the southeast side of the WG. In section 4, we try to correlate the shape and size variability of the WG with inflow variations through the Strait of Gibraltar induced by atmospheric pressure variations over the western Mediterranean and with the internal hydraulics of the Strait. Finally, Section 5 summarizes in cartoon-like form what, in our opinion, could have happened during the 15-day survey period.

2. Data

The ICTIOALBORAN-0793 oceanographic survey was carried out on the RV *Francisco de Paula Navarro* of the Instituto Español de Oceanografía (IEO) from 8–26 July 1993. Each station (Fig. 1) consisted of a CTD cast plus ichthyoplankton hauls and water samples to evaluate nutrients (these last data have not been used here). Satellite images covering the period of the survey, sea level data in the Strait of Gibraltar and atmospheric pressure data complete the analysed information.

2.1. CTD

A "SBE-25" CTD probe was used. In addition to conductivity, temperature and depth sensors it measured dissolved oxygen, fluorescence, pH and active photosynthetic radiation. Only the first three are of concern for us in this paper. The probe was lowered to a maximum depth of 210 m to avoid damage to certain sensors. Data were filtered to obtain 1 m interval sampling. Salinity was evaluated using the practical salinity scale (PSS) and density calculated from the revised state equation of Millero and Poisson (1981).

2.2. Ichthyoplankton sampling

A "Bongo-40" net, equipped with two independent flow meters "General Oceanic 2030" and one depth-meter gauge, was employed to carry out "double-oblique" trawls from the surface to 100 m depth. Mesh sizes of 250 μm (to determine the zooplankton biomass) and 350 μm (to make the taxonomic identification of the ichthyoplankton) were used.

2.3. Satellite imagery

Thermal imagery covering the survey period was processed from the advanced very high resolution radiometer (AVHRR) sensor onboard the NOAA-11 satellite. We present channel 4 bright temperature imagery instead of corrected sea surface imagery because the resulting multichannel sea surface temperature images are of poor quality (increased noise levels and reduced sea surface temperature gradients) in comparison with the imagery of the original channels 4 and 5 (La Violette and Holyer, 1988). Well-defined temperature gradients are necessary to give some clues about the underlying dynamics. The geometrical correction was made using the localization points on the earth's surface (deduced from the ephemerides of the satellite). The final images, a representative selection of which are presented in Fig. 7, have about a 1 km resolution. Temperatures from the images were checked against *in situ* CTD data taken on the same dates. Thermal images systematically give temperatures 1.5°C higher than CTD. The fact that the uppermost CTD sample was 2 m below the sea surface can account partially for the discrepancy. Another cause could be the skin effect (diurnal heating) when the image was taken during daylight, but similar differences were observed when they were taken at night. Since the bias is rather regular, we have considered the thermal structures on the images as indicative of the underlying dynamics.

2.4. Atmospheric pressure

Daily atmospheric pressure averaged over the areas of the Gulf of Cadiz (west of the Strait) and western Mediterranean was collected from the daily bulletin of Instituto Nacional de Meteorología, Spain, during July. The values were obtained from synoptic maps that represented the weather situation at 12:00 GMT and then smoothed with a filter of weights 0.25, 0.5, 0.25.

2.5. Sea level

Hourly sea level values at Ceuta and Algeciras (south and north shores of the Strait; Fig. 1) during July 1993 were obtained from the tide network installed and maintained by IEO in the Strait of Gibraltar. The values were filtered by the tide-killing filter C51 designed by Groves (1955), which has an excellent response for eliminating tidal signals (they are filtered out by more than 99.4 and 99.99% in semidiurnal and diurnal bands, respectively). The resulting tide-free sea level heights were sub-sampled to have daily values centred at noon.

2.6. Synopticity of survey data

The duration of ICTIOALBORAN-0793 was 19 days, too much to consider the data as synoptic. Up to now there has not been an intensive field experiment long enough to determine a reliable time-variability scale, but there are some indications aiming at a time scale on the order of a few days. For instance, Perkins et al. (1990),
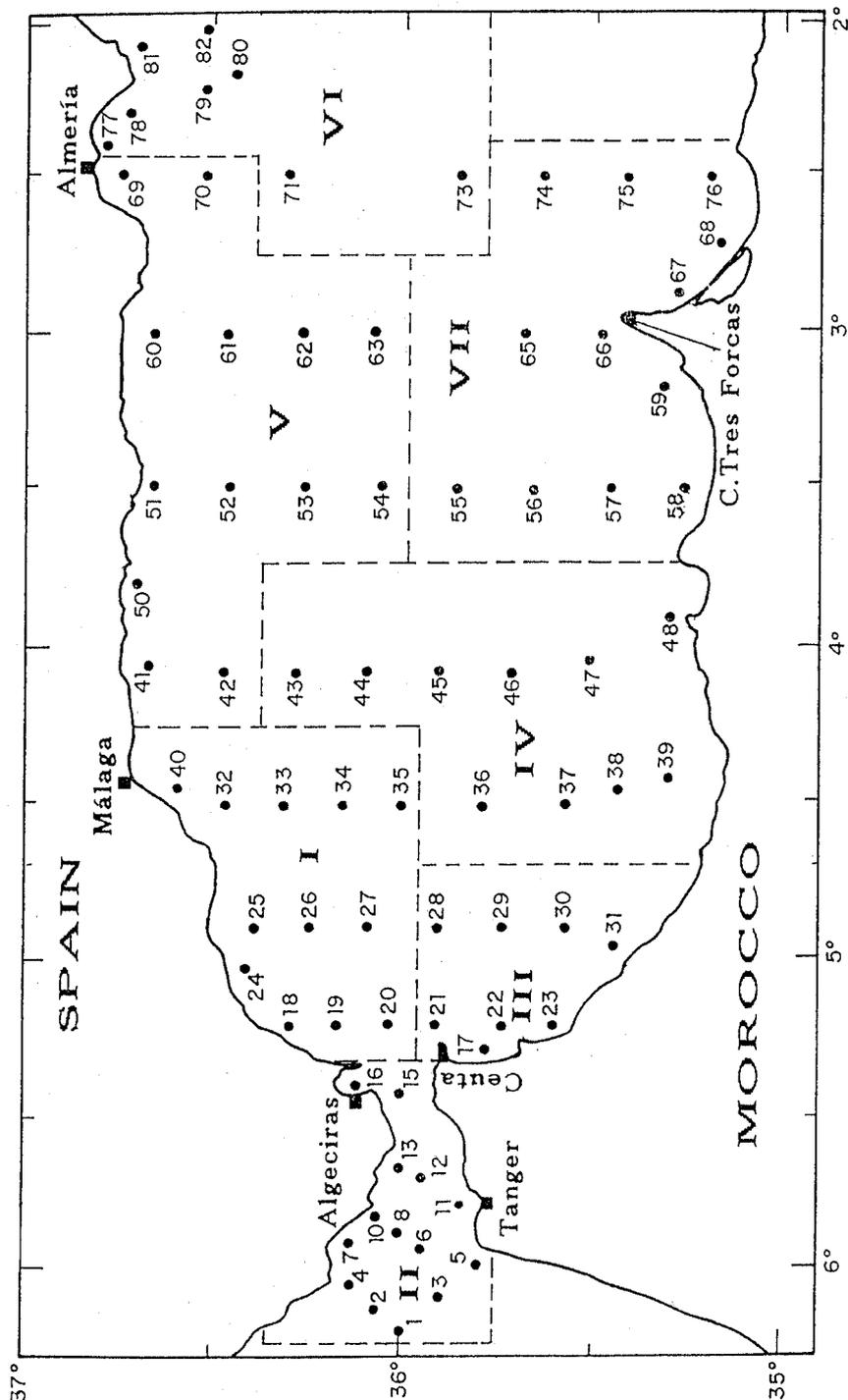
Fig. 1. Alboran Sea map showing the locations of the oceanographic stations of the ICTIOALBORAN-0793 cruise. The map is divided into boxes according to the dates on which stations were occupied (see text and Table 1). Data within each box are considered synoptic.

from plots of currents taken along a north–south section of the Western Alboran Sea, show the existence of pseudo-periods of about 9 days. La Violette (1984) was able to identify sub-mesoscale features advected by the Jet at typical speed of 0.4 m s^{-1} from a set of satellite images, which implies displacements in the order of the basin dimensions (O(100 km)) in a 6-day period. Mesoscale variability is also expected to be shorter than the length of the survey. Macroscale field (what we could call quasi-permanent features) may have longer time scales. For example, Viudez et al. (1996) did not find significant variations in this field after examining a set of infrared images covering the period of their experiment (22 September–7 October 1992). During our survey, things appeared to have been different. Because of the lack of simultaneity in our sampling and to avoid misunderstandings we have divided the whole period into sub-periods of 2 days (exceptionally 3). Fig. 1 shows the "boxes" resulting from this division. Each box groups stations according to the dates when they were occupied (Table 1) and shall be considered synoptic. Box II has not been included in our analysis due to the high-frequency (tidal) variability in the Strait of Gibraltar.

The above considerations are important. For instance, the dynamic topography shown in Fig. 2 was done by including all data of the survey as if they were synoptic. The resulting WG is obtained from data in box I (sampled around 9 July) and boxes III and IV (13–16 July). Judging from the satellite images presented in Fig. 7, conditions during both periods were significantly different. Fig. 7(a) is representative of the period when box I was sampled, and Fig. 7(b) may be adequate for boxes III and IV. To consider these data as synoptic, it is equivalent to superposing different situations in order to build a unique rather "artificial" WG. Some clues to this performance are seen in Fig. 2: the outcropping of isolines in the north part of the gyre (inside box I) indicates a strong flow similar to that suggested in Fig. 7(a); the smooth topography in the centre of the gyre is in accordance with a larger WG, like the one in Fig. 7(b). Another example of discrepancy is presented below. However, figures like Fig. 2 are useful as long as we consider stations inside each box. For instance, geostrophic calculations in the north part of the gyre give correct estimations of the geostrophic velocity, since it is inside box I, but the resulting value is representative only of the dates when the box was sampled.

Table 1
Chronology of the survey. The different boxes correspond to the division shown in Fig. 1

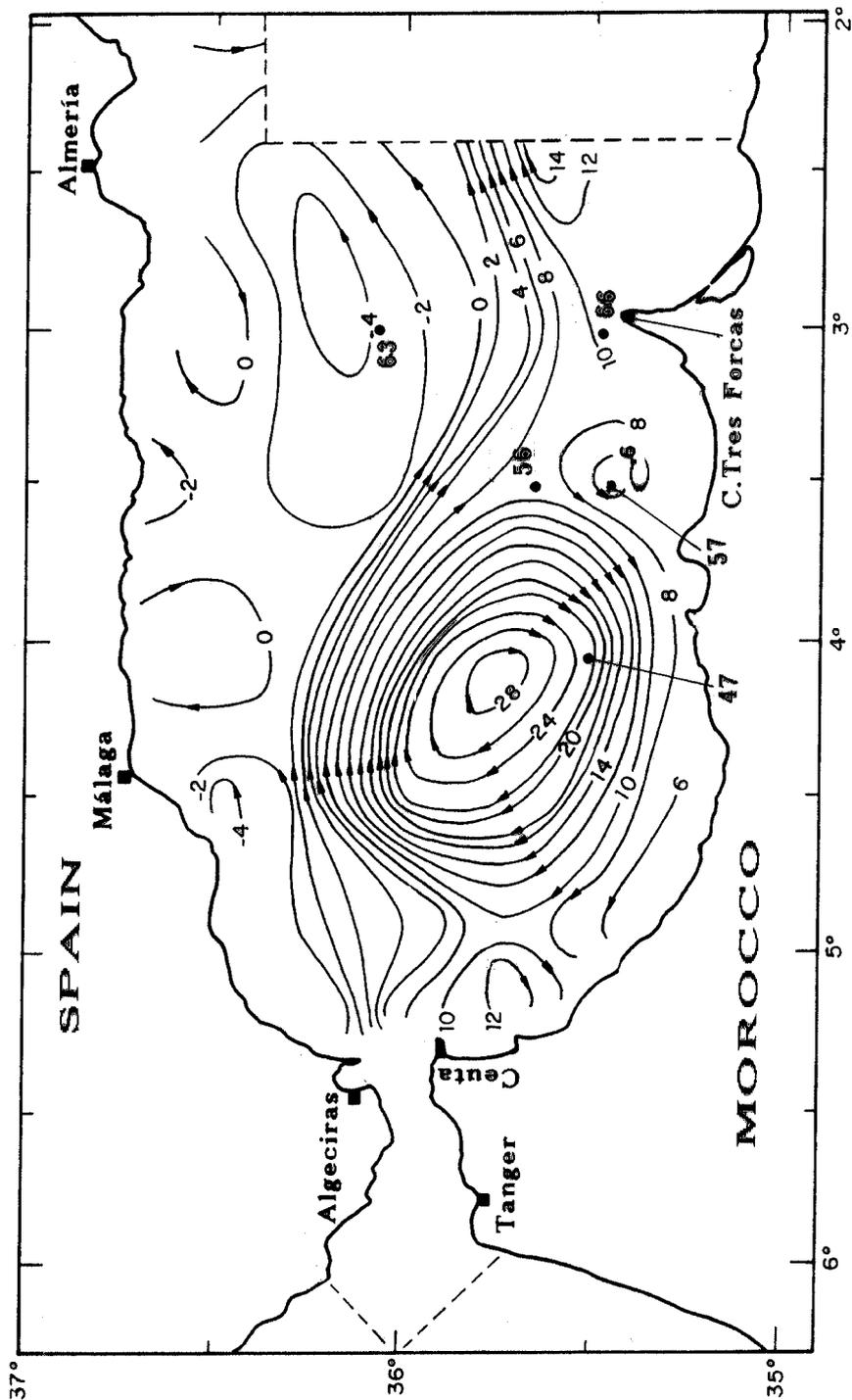| Box	Days of sampling (July 1993)
I	8, 9
II	10, 11
III	13, 14
IV	15, 16
V	18, 19, 20
VI	21, 22
VII	24, 25, 26

Fig. 2. Dynamic topography inferred from the whole dataset of the cruise. Cyclonic eddy "C" west of Cape Tres Forcas is marked. Some stations of special interest are also marked.

3. Data interpretation

3.1. Cyclonic eddy "C"

West of Cape Tres Forcas a small cyclonic eddy was observed ("C" on Fig. 2). The core consisted of a mass of water saltier and warmer than the water around it (Fig. 3). This fact is more apparent in Fig. 4(A) if we compare the T–S characteristics of five selected stations (see Fig. 2 for their location). Station 57, at the centre of the eddy, has T–S characteristics closer to Station 63 in the northern part of the basin than to its neighbour station 47 and, particularly, Stations 56 or 66. Temperature and salinity profiles at Stations 56, 57 and 58 (Fig. 4B) allow us to estimate a thickness of 35–45 m of anomalous (salty and warm) surface water in the eddy (Station 57) compared with the (Atlantic) surface water at Stations 56 and 58, north and south of it. The water of the surface layer of the eddy was of the same type as that in the northern part of the Alboran Sea (we will call this water Mediterranean Surface Water (MSW), a water warmer and saltier than the just arrived AW due to its time of residence in the
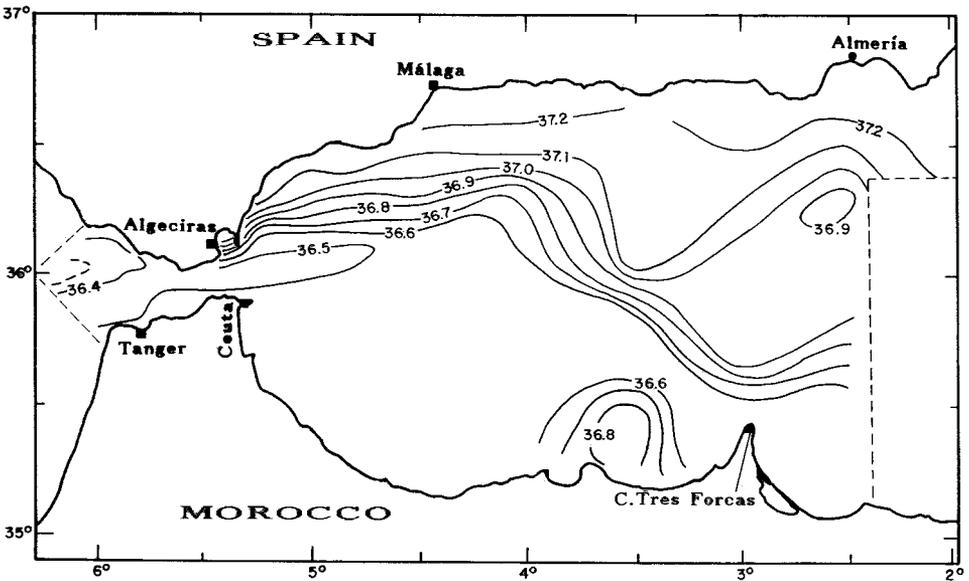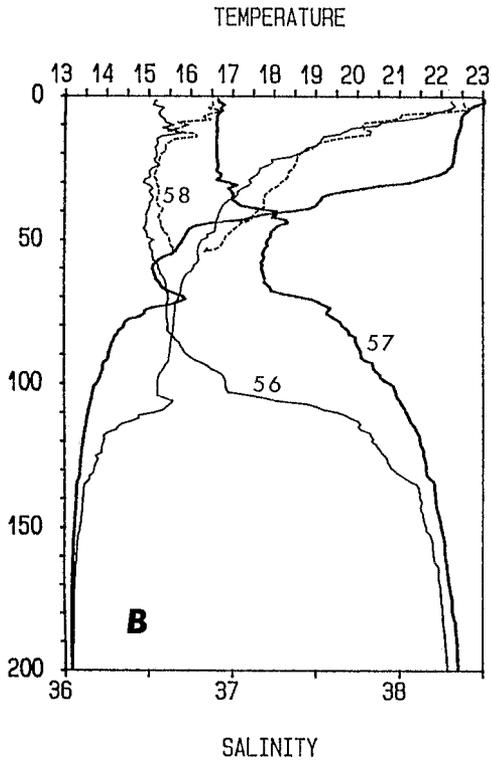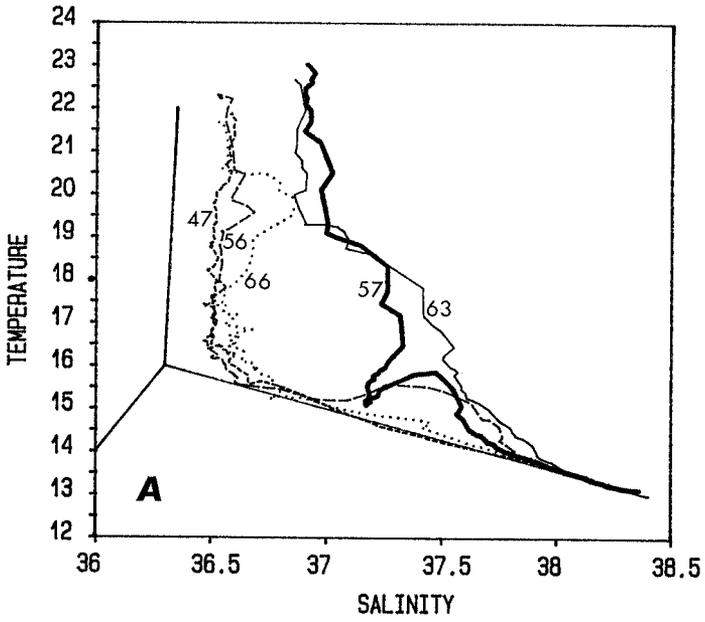

Fig. 3. Salinity at 10 m depth. Note the high salinity core at the position of eddy "C".

Fig. 4. (A) T–S diagrams of stations marked on Fig. 2. (B) Salinity and temperature profiles at Stations 56 (thin, full line), 57 (thick, full line) and 58 (dashed line). Surface waters at Stations 56 and 58 are very similar, while Station 57, between them, has different water characteristics.
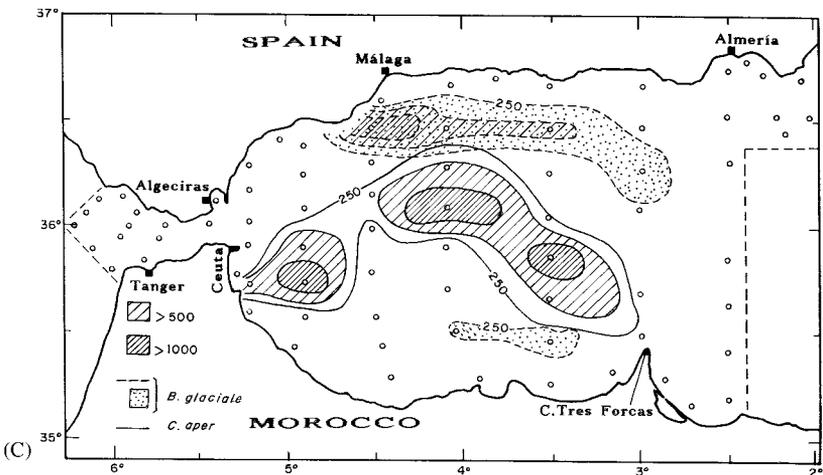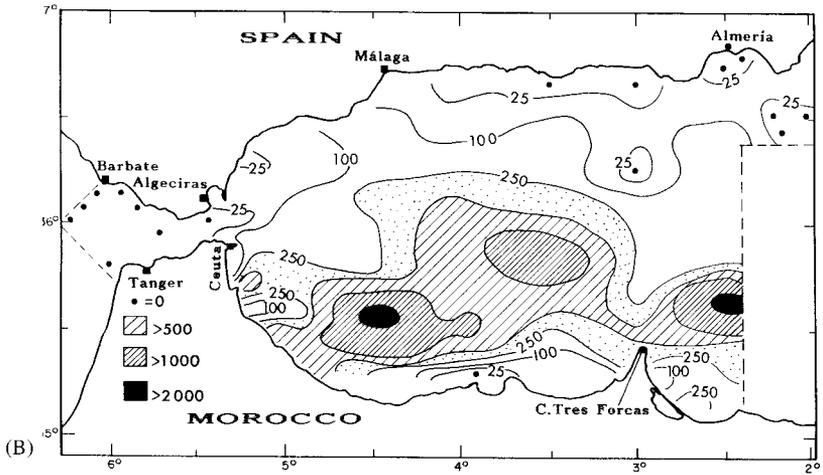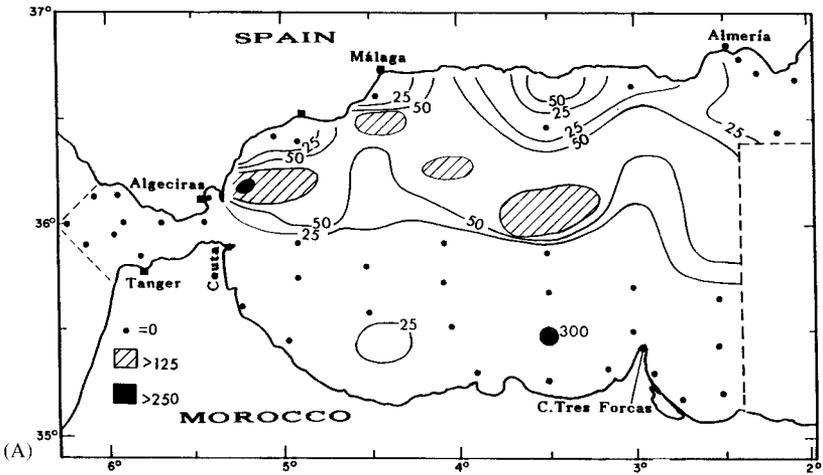
Mediterranean Sea). Biological tracers also confirm its origin. Fig. 5(A,B) represent fish larvae concentration of *Maurolicus muelleri* and *Ceratoscopelus Maderensis*, respectively. The first species abounds in the northern Alboran Sea but its concentration was high in eddy "C". The second species dominates the southern half of the basin; however, the concentration in the eddy area was much lower than in other southern stations. Even more clarifying is Fig. 5(C): larvae distribution of *Capros aper* (species often found in summer sampling of coastal ichthyoplankton) spread over the Atlantic Jet area in the Western Basin. North of the Jet, large amounts of larvae of *Benthosema glaciale* (mesopelagic species of Arctic-boreal nature which lives in the Alboran Sea) were found. But significant amounts of them were also present in the eddy on the other side of the Atlantic Jet which, in fact, represented a physical barrier for the motion of these larvae.

   Most of the stations used to identify the eddy were inside box VII. Furthermore, the stations inside the box that helped define it were accomplished in a time span of less than 21 h. We also realize that the easternmost stations of box IV, made some days before, were necessary to define it and, as a result, controversy may arise about its actual existence. We argue that these last stations are well inside what we can call the "permanent WG area" and, despite the fact that their dynamic heights when box VII was sampled may differ from the heights in Fig. 2, whatever their values may be, we believe they are of the same order as in Fig. 2 or in any case greater than the value at Station 57, the centre of the eddy. Moreover, the important question here is to realize that the eddy was isolated from its source by the Atlantic Jet and that this result has been directly deduced from data fully inside box VII. So, we conclude that eddy "C" was a true result and not a spurious result arising from the lack of simultaneity. It is also convenient to say that it was found in a region where positive relative vorticity has often been reported by several authors (Cano, 1977; Villalobos et al., 1989; Tintore et al., 1991; Viudez et al., 1996). Cyclonic circulation here is not surprising if we consider the path followed by the Atlantic Jet in the Western Basin: after going around the north and eastern part of the WG, it impinges against the African coast, splitting into two veins, the one to the west to be incorporated into the WG (Whitehead, 1985; Gleizon, 1994), the other to the east or northeast following the African coast, thereby describing a pronounced cyclonic meander. MSW would be at the northern side of this vein and AW to the south. The situation during our survey seemed to be a more evolved one, since MSW was south of the vein, suggesting eddy shedding from the meander. Moreover, this detachment had to take place some time between the beginning of the survey and the date when box VII was sampled: surface temperature distribution from Fig. 7(a) of 11 July (21°C) indicates that the eddy was not formed yet, since the measured surface temperature was 23°C (Fig. 4a,b), a value

Fig. 5. Larval concentration distribution (larvae/10 m^2) of *Maurolicus muelleri* (A), *Cerastocopelus maderensis* (B) and *Benthosema glaciale* and *Capros aper* (C). Note the anomalous distribution of the first three species in the area of eddy "C". Larval concentration at Station 57 in (A) is explicitly displayed, since this discrete sample is not suitable for contouring.

compatible only with temperatures inferred from Fig. 7(d) of 22 July ($\geqslant 24°C$), taking into account the 1.5°C of bias already mentioned. Box VII was sampled around 25 July.

3.2. Atlantic water in the cores of the anticyclonic gyres

Fig. 6(A–C) are salinity sections across the WG, 3°W and the EG, respectively. Although the size and extension of the EG cannot be defined from our sampling, the dynamic topography of Fig. 2 suggests a rather small EG and, if so, the section across 2.5°W must be close to the centre of the gyre. Fig. 6(A and C) show the presence of water whose salinity is less than 36.5 in the core of both gyres. If the AW Jet enters the Alboran Sea due east and does not describe a large meander in the Western Basin, then it needs about 4 days to get the EG from the Strait of Gibraltar if we assume a moderate speed of 0.7 m s^{-1}. Under these circumstances, the AW that enters the Eastern Basin would have salinity of 36.5 or less (Atlantic value) since it has not had time to lose its signature by mixing or evaporating along its path from the Strait. Thus, it is not surprising to find water of $S \leqslant 36.5$ in the core of the EG too. But when the 3°W section was made, salinity values as low as these were not found (Fig. 6B). This is an unexpected result since the low salinity water in the core of the EG had to cross this section, mainly between Cape Tres Forcas and Alboran Island. Even more surprising is to observe that the vein of the Jet entering the Eastern Basin (thick lines in Fig. 6B) transported water whose salinity was close to 37.0 when, supposedly, the vein should have supplied the low salinity water to feed the EG. In our opinion, the flow of low salinity water through the 3°W section was interrupted some time before box VII was sampled and replaced by a mixing of it and MSW.

3.3. Time evolution from infrared imagery

Eddy "C", whose hydrographic and biological characteristics are atypical in view of its geographical location, had to arrive there as a consequence of an evolutionary process. To investigate it we have analysed the set of thermal images presented above. The first image shows a well-defined and not too large WG, bounded at the north by an apparently robust Atlantic Jet, due east, which follows a smooth path along the Western Basin. In Fig. 7(b), the Jet has been deflected northeastward by a WG that has increased its size and occupies the basin breadthwise (north–south direction), allowing a vein of MSW to be dragged southward along the eastern edge of the gyre. Fig. 7(c) shows an intrusion of cold AW through the Strait in an eastward direction, "collapsing" at a right angle with the WG at its western edge. The image suggests a flooding or replacement of the existing gyre by this just incoming cold and, presumably, fast flow. Next Fig. 7(d) illustrates this process in a more evolved stage: the "old" gyre has been pushed eastward and stretched, favouring the southward penetration of MSW, whose "head" now occupies the position in which eddy "C" was found three days later. Fig. 7(e) shows a situation similar to the second one. As an
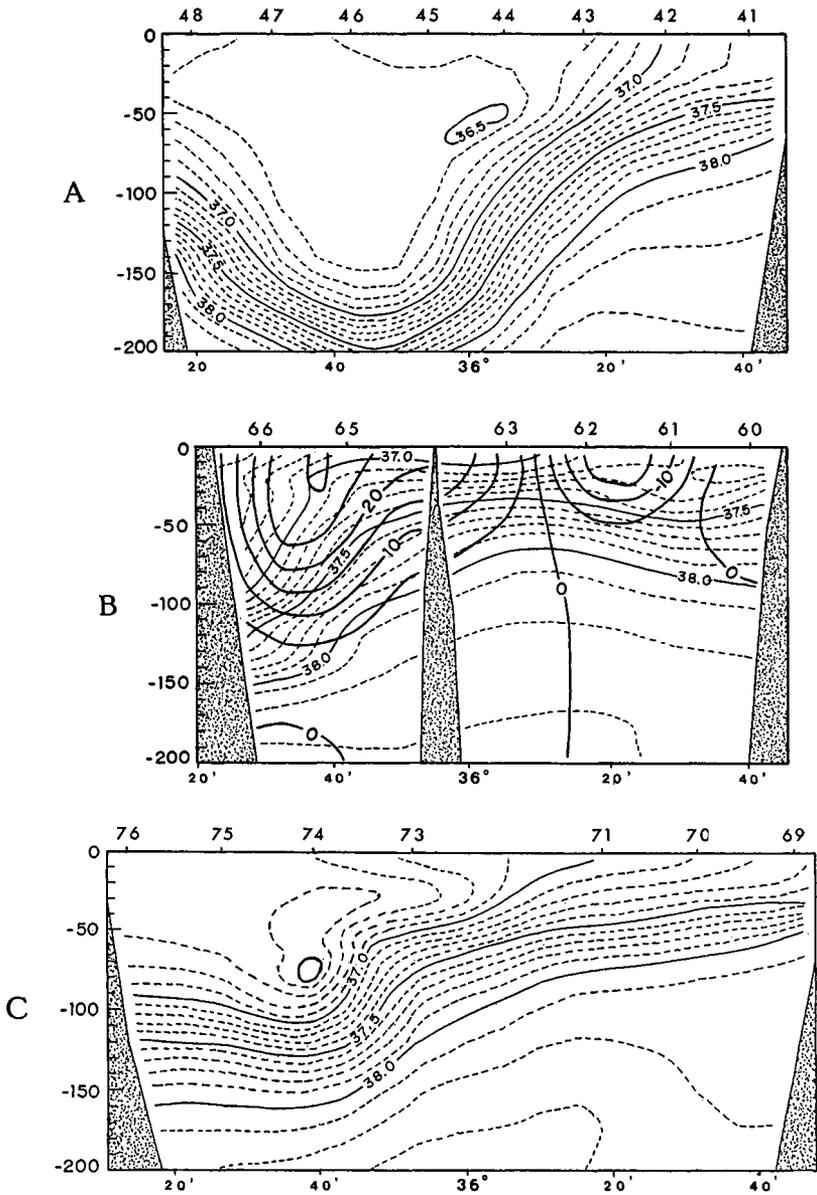
Fig. 6. Salinity profiles through: (A) 4°W section, which cut through the WG; (B) 3°W, including the passage between Alboran Island and Cape Tres Forcas; and (C) 2.5°W, through the EG. Thick lines in (B) represent the zonal geostrophic velocity, positive eastward.
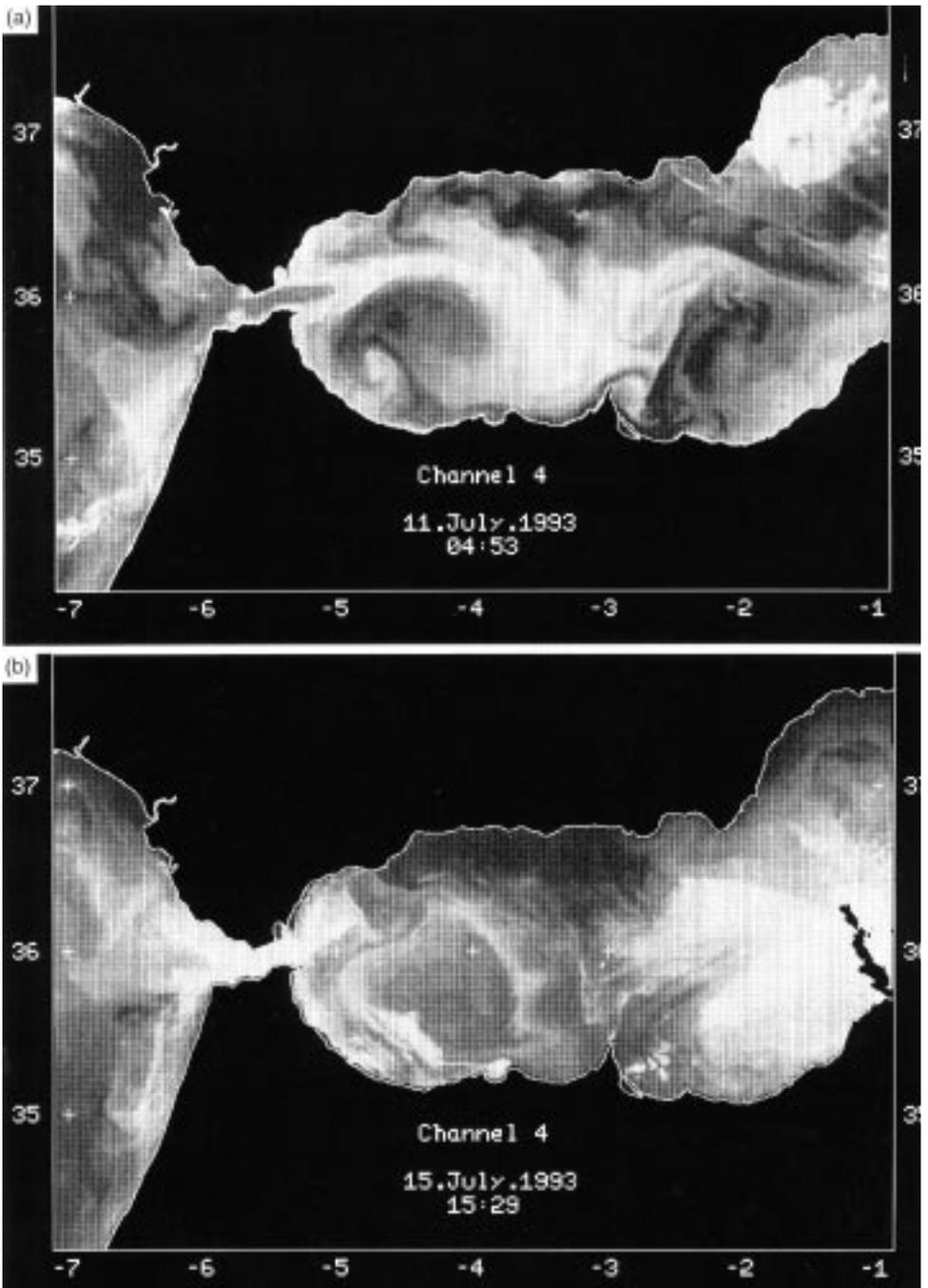
Fig. 7. Sequence of selected infrared images taken during the cruise. Dates are shown on the images. Dark (light) tones correspond to warm (cold) water,
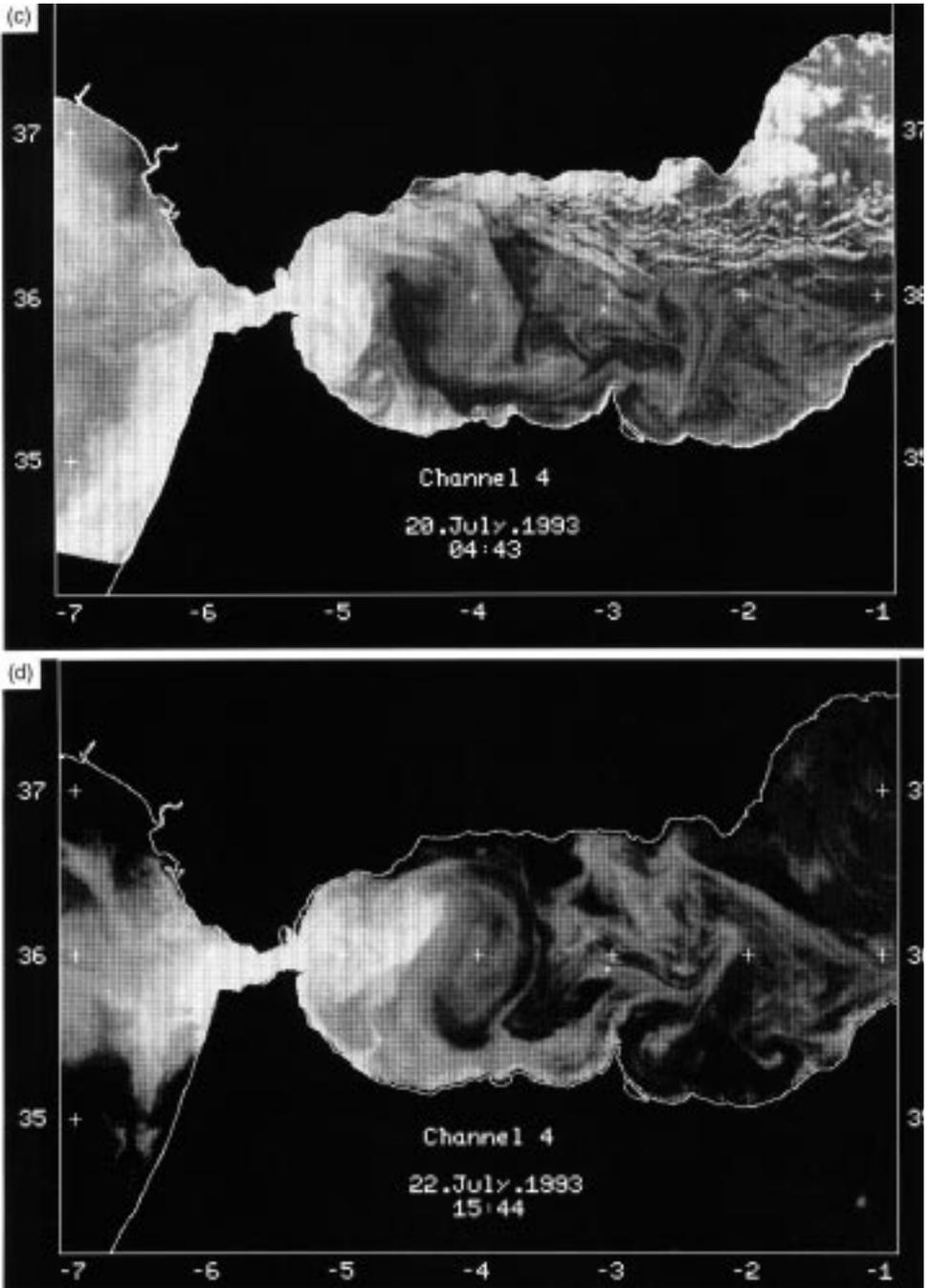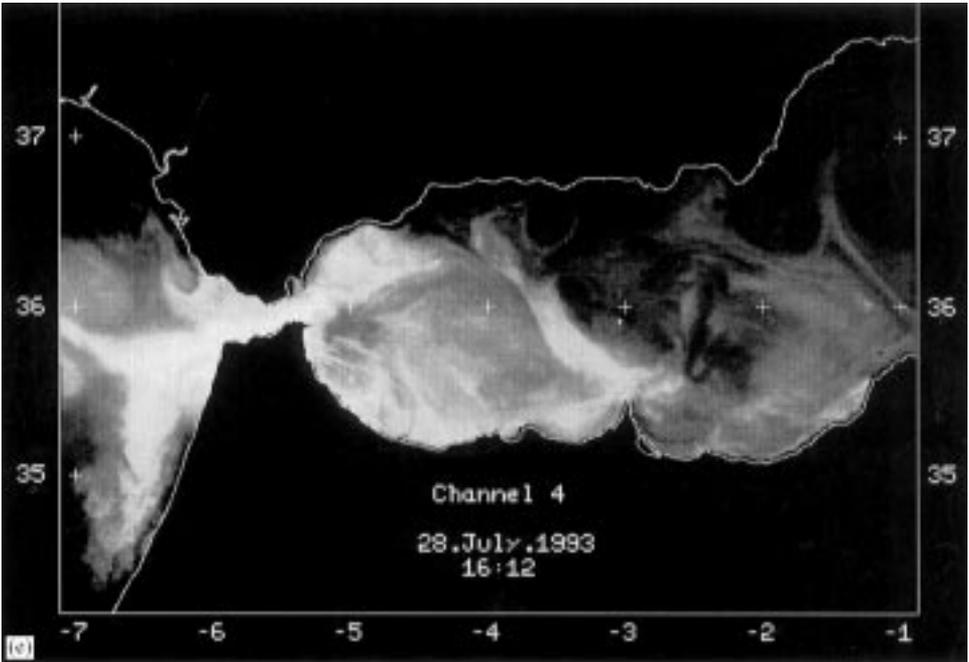
Fig. 7 (*continued*)

Fig. 7 (*continued*)

anonymous referee of this paper pointed out, it is noteworthy that other works dealing with variations in the surface circulation inferred from satellite imagery (La Violette, 1984; Heburn and La Violette, 1990, for instance) present sequences of images that could support our interpretation and suggest that the evolution explained above could be more usual than expected.

The evolution above is also in agreement with observations of eulerian currents presented in the already mentioned work of Perkins et al. (1990), the best dataset of currents taken in the Alboran Sea. They report counterclockwise rotation for all velocity records taken in the upper 100 m layer along the "Marbella section", as they called it, a section with five mooring lines, the first and northernmost one near the Spanish coast, the last one slightly to the south of 36°N (Stations 25, 26 and 27 in our Fig. 1 are more or less at the same position as their section). According to them: (1) southern moorings led northern ones, indicating a northward phase propagation of the eastward velocity of the Jet–WG system; (2) counterclockwise rotation prevails, meaning that a current initially directed eastward becomes gradually more northward with the periodicity shown in their rotary spectra; (3) the inflow goes farther eastward when its speed is greater and more northward as it weakens; and (4) they observe a tendency of events to begin at the south of the mooring array and to end at the north. They also suggest a redevelopment of inflow in the eastward direction.

4. Variability of the WG and Atlantic inflow

4.1. Some simple considerations

The equation for horizontal velocity of an inviscid fluid in a rotating system can be written as:

$$\frac{d\overline{v_h}}{dt} + f\overline{k} \wedge \overline{v_h} = - \nabla_h \phi \tag{1}$$

where sub-index h stands for "horizontal", ϕ is the dynamic height, $\overline{k}$ is the vertical unit vector, and the remaining symbols have their usual meaning. Let us consider a gyre of circular shape bounded by a Jet (see sketch in Fig. 8A). For this geometry, it is more convenient to write eqn (1) in cylindrical coordinates, the origin at the centre of the gyre. The projection along the radial coordinate gives

$$\frac{\partial V_r}{\partial t} - \frac{V_\theta^2}{r} - f V_\theta = - \frac{\partial \phi}{\partial r} \tag{2}$$

where sub-indexes r and θ stand for radial (positive outwards) and azimutal (positive anticlockwise) coordinates. Under stationary conditions ($V_r = \text{constant} = 0$), eq (2) reduces to the gradient current equation $(V_\theta^2/r) + f V_\theta = (\partial \phi/\partial r)$ or the geostrophic one $f V_\theta = (\partial \phi/\partial r)$ if we ignore centrifugal acceleration. Let us suppose that the Jet at the north part of the gyre (see Fig. 8A) changes its speed (due to a change in the speed of the inflow through the Strait, for instance). If we assume that, initially, ϕ gradient has not changed yet, neither the gradient current equation nor the geostrophic one can be satisfied and a radial acceleration given by:

$$\Delta\left(\frac{\partial V_r}{\partial t}\right) = \left(f + \frac{2V_\theta}{r}\right)\Delta V_\theta \tag{3a}$$

or

$$\Delta\left(\frac{\partial V_r}{\partial t}\right) = f\Delta V_\theta \tag{3b}$$

must appear, depending on whether or not we consider centrifugal force. This will change ϕ gradient until a new balance is achieved. Let us consider an increase of the speed. Since V_θ is positive anticlockwise, the increase of the speed implies $\Delta V_\theta < 0$; the expresion inside brackets in eqn (3a) is positive as far as $|V_\theta| < R_0 f/2$, R_0 the radius of the gyre, or $\varepsilon = |V_\theta|/R_0 f < 1/2$, ε being a Rossby number adequate for our geometry. We expect that this condition is always satisfied (despite the fact that Fig. 2 does not represent a synoptic situation, it is still useful to estimate a value for ε: let R_0 be the distance necessary for ϕ to pass from ϕ_0, its maximum value at the centre of the gyre, to 0 at the periphery. V_θ will be adimensionalized by $U_0 = \phi_0/fR_0$ and the Rossby
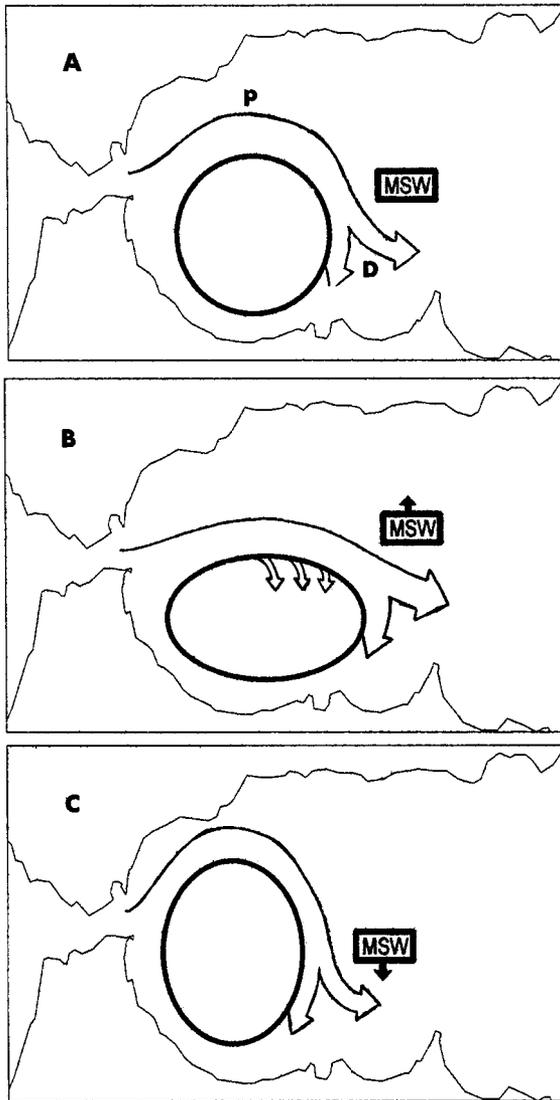
Fig. 8. (A) An idealized steady situation with a circular shape of WG encircled by a jet in geostrophic balance. The jet is forced by topography to split into two veins at point "D". MSW is north of the meander. (B) Likely evolution of the system after an increase of the jet speed takes place at point "P". Surface AW can flood the eastern part of the gyre and occupy the area west of Cape Tres Forcas. MSW is pushed to the north. (C) Same as (B), but after a decrease in the speed of the jet at "P". The gyre stretches in a north–south direction and MSW can proceed further south.

number will be given by $\varepsilon = \phi_0/(R_0^2 f^2)$. With, $\phi_o = 29$ cm dyn $= 2.9$ m^2 s^{-2} and $R_0 \approx 55$ km, we obtain $\varepsilon \approx 0.13$), so that $\Delta(\partial V_r/\partial t) < 0$ regardless of the equation we use. Thus, an increase in the speed will be followed by a southward drift of the Jet. Fluid particles would be deflected to the south tending to flood the gyre. The perturbation produced at the northern edge will propagate with the speed of the first internal baroclinic mode ($c \approx 1.5$ m s^{-1} for a two layer sea with $\Delta\rho = 2.5$ kg/m^3 and an upper layer depth of 100 m) plus the advection velocity, stretching the gyre in a west–east direction. The final result would be a spreading of the Jet over the westernmost area of the gyre (sketched in Fig. 8B), a situation strongly suggested by image 7a. The MSW that would have been in this area would be displaced northward. Conversely, if the speed is reduced, $\Delta V_\theta > 0$ and $\Delta(\partial V_r/\partial t) > 0$ always. Fluid particles will be pushed outwards to the north causing the gyre to be stretched in a north–south direction in the way outlined in Fig. 8(C) (image 7b could be illustrative). A laboratory model by Gleizon (1994) shows this evolution too. Under these circumstances, the MSW can penetrate to the south and the gyre–Jet system would evolve to a new situation that will be achieved by evacuating or incorporating water to match the new size. A natural time scale to measure this process would be the time needed by a fluid particle to go around the gyre, that is, 3–4 days for conditions shown in Fig. 2. Shorter variations of V_θ will probably be filtered out.

The scenario we have depicted is very simplified but agrees with what the images of Fig. 7 suggest. Next, we will see that it is also consistent with inflow variations through the Strait.

4.2. Time variability of the Atlantic inflow

The forcing mechanism for the Alboran Sea surface variability must be the velocity variations of the Atlantic inflow through the Strait. The inflow is in a quite good cross-strait geostrophic balance at the eastern section of the Strait of Gibraltar (see Kinder and Bryden, 1987, particularly figure 3 of their work). Measurements of cross-strait sea level slope can be used to estimate an averaged inflowing speed U according to:

$$U = \frac{g\Delta\zeta}{f L} \tag{4}$$

where $(\Delta\zeta/L)$ is the cross-strait slope, $\Delta\zeta$ being the sea level difference between two points separated a distance L. The lack of accurate levelling between both sides of the Strait makes the estimation of U from Eq. (4) scarcely reliable. In other words, an unknown constant must be added to its right-hand side. But variations of U due to variations of $\Delta\zeta$ are correctly predicted since the constant term cancels. Fig. 9(A) shows the difference of sea level between Ceuta and Algeciras. Labeled crosses have been included to show the moments when satellite images in Fig. 7 were taken. The most outstanding feature is the large drop of $\Delta\zeta$ between 11–16 July, implying a considerable diminution of U according to Eq. (4). For a $\Delta\zeta$ drop on the order of 8 cm and taking $L = 18$ km, U decreases by 0.5 m s^{-1}, a large variation indeed. It is

worthy to note that image 7a was taken on 11 July and image 7b on 15 July. Velocities deduced through sea level slopes from Fig. 9(A) support the interpretation made above.

On time scales of a few days (subinertial frequencies) the driving force for inflow variations is the atmospheric pressure variations over the Mediterranean Sea, particularly over its Western Basin (Candela et al., 1989). Fig. 9(B) shows Δp_a, differences of (daily) atmospheric pressure over the Gulf of Cadiz and Western Mediterranean. The similarity to Fig. 9(A) is obvious. However, the correlation coefficient between both series is only 0.48, less than expected. The reason is that fluctuations do not correlate by the middle of July (the value increases to 0.80 for the first 12 days and to 0.75 for the last 14 days). Data in Fig. 9(B) show a dominant period of 5 days for the fluctuations, a result confirmed by spectral analysis of longer series taken in summer. Candela
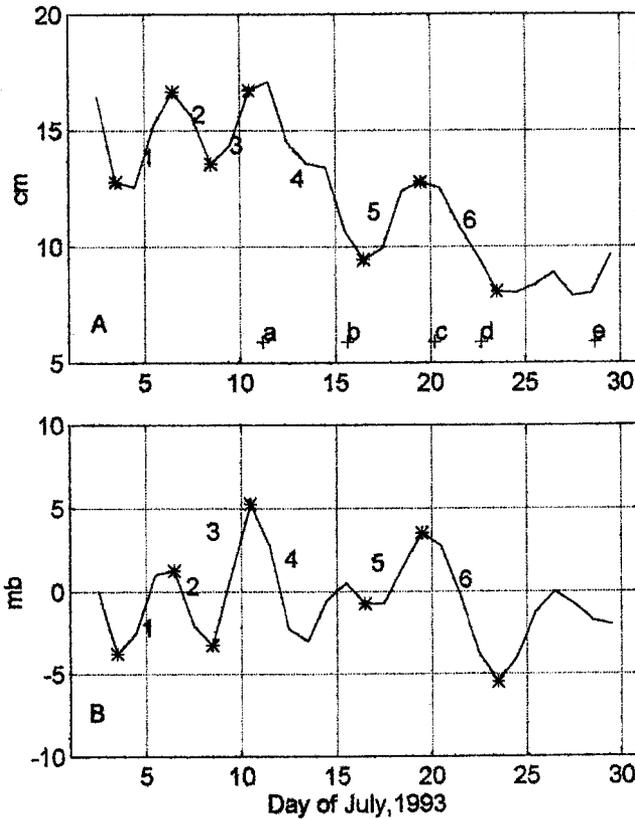

Fig. 9. (A) Cross-strait sea level differences (south side, Ceuta, minus north side, Algeciras). Labels a–e indicate the dates of satellite images. Labels 1–6 identify events that are studied in Table 2. (B) Atmospheric pressure differences (mb) between the Gulf of Cádiz and the western Mediterranean Sea. Labels 1–6 have the same meaning as in (A).

et al. (1989), study the gain and phase functions between sub-inertial barotropic fluctuations of transport through the Strait of Gibraltar and the atmospheric pressure over the Mediterranean Sea; for $0.008 \, \text{c h}^{-1}$ (5 days) they are $0.08 \, \text{Sv mb}^{-1}$ and around $180°$ (the sign of Δp_a in their work was opposite to ours). In general, we may say that barotropic fluctuations deduced from Δp_a via Candela's model agree well with U fluctuations deduced from $\Delta \zeta$ via Eq. (4). However, from 11 July to 16 July the model fails since a small Δp_a variation is followed by an unreasonably large $\Delta \zeta$ drop. Before proceeding further, we have considered the possibility that this drop was due to errors in sea level data similar to those described in Garrett et al. (1989). We carried out an analysis similar to that explained in their paper and we have not found any anomaly. Thus, we consider this drop to be dynamically significant. Candela's model gives transport fluctuations, not U variations. Transport and velocity are linearly correlated only when the thickness of the inflow remains unaltered. The layer thickness as well as other properties of the inflow (even the value of L in Eq. (4)) depends on the internal hydraulics of the Strait.

4.3. A tentative interpretation

Hydraulic models of the Strait of Gibraltar, which reproduce rather well the baroclinic exchange through it, predict two different states for the exchange: maximal and submaximal (see Bryden and Kinder, 1991 for a good description of these theories). The first situation corresponds to supercritical flow of AW at the easternmost section of the Strait, that is, a thin layer of AW moving at high speed. Earth rotation causes the flow to separate from the Spanish coast some kilometres before reaching the easternmost section of the Strait (Bormans and Garrett, 1989a) and the streamlines can be slightly deflected clockwise, so that they do not follow the axis of the Strait, as suggested by Fig. 11.1 and 11.2 of the work by Armi and Farmer (1988). Similar deflexion of streamlines in hydraulically controlled flows over weirs in rotating fluids have been seen in laboratory experiments (Sambuco and Whitehead, 1976). Thus, the flow enters the Alboran Sea in an almost eastward direction or at least with an angle less than $17°$, the orientation of the axis of the Strait. This situation is strongly suggested in Fig. 7(a). Flow separation also implies a decrease in the value of L in Eq. (4), which, together with the high speed associated with a supercritical regime, gives large values for $\Delta \zeta$. Furthermore, a supercritical flow isolates hydraulically the Jet in the Strait from the downstream basin, and conditions in the Alboran Sea cannot affect its properties, such as the incoming direction or speed. Submaximal exchange, on the other hand, implies sub-critical flow at the eastern section or a thicker layer moving slowly, attached to the Spanish coast. Bormans and Garrett (1989a) show that earth rotation has a small effect on the flow, which translates into negligible deflection of streamlines that now would follow the axis of the Strait. Under these circumstances, $\Delta \zeta$ is lesser than before. Conditions in the downstream basin can influence the flow in the Strait as, for instance, the incoming angle: the flow can be deflected to the northeast by a growing WG. Laboratory simulations in which the inflow is kept sub-critical (Gleizon, 1994) lead to the formation of a large WG that has tendency to
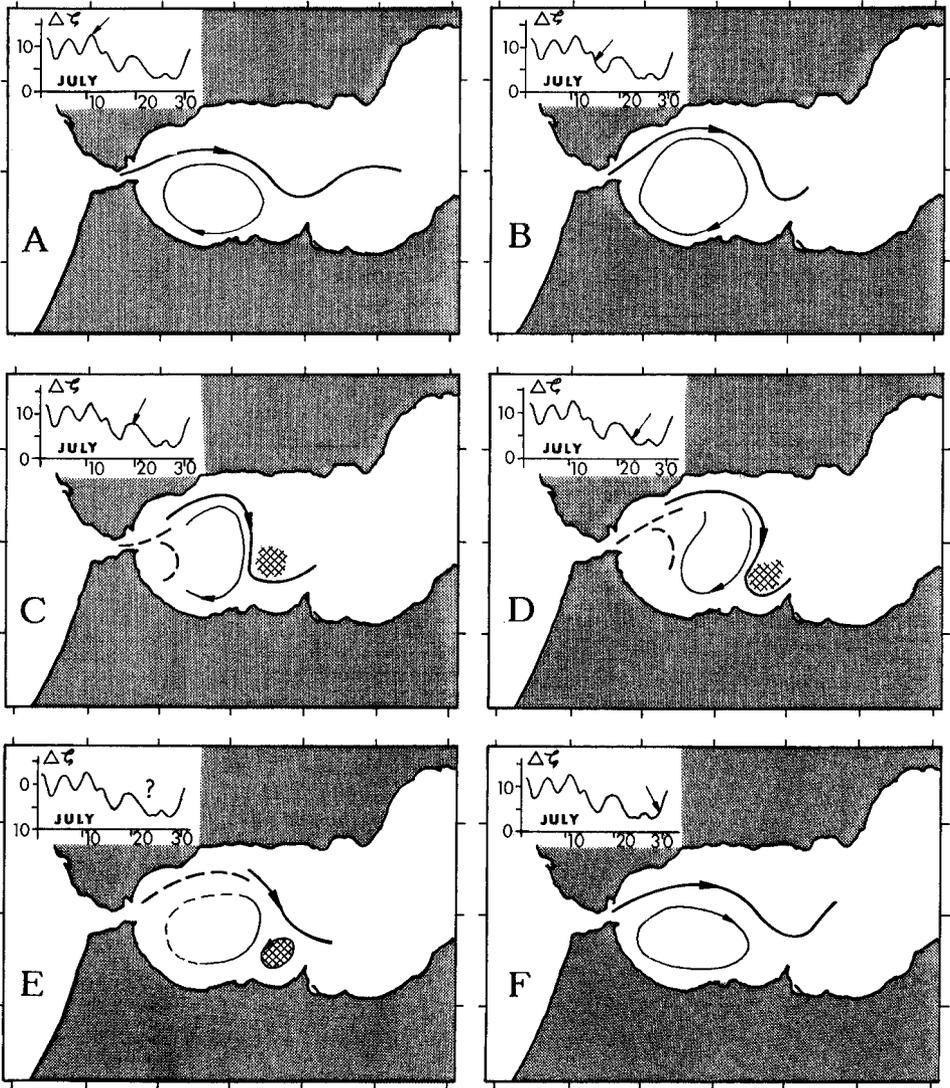
Fig. 10. Synopsis showing the likely time evolution of the observed structures in the Alboran Sea during the cruise. All figures except (E) are based on infrared images shown in Fig. 7. The upper corner on each "snapshot" shows a reproduction of Fig. 9(A), with the arrow pointing at the date corresponding to the image. Full lines indicate the jet (thick) and gyres (thin); dashed lines have the same meaning but refer to the latter intrusion of colder AW commented on the text.

grow until it occupies the whole north–south extension of the basin, in a way very much like that of image 7b.

Large variations of the inflowing speed do not necessarily imply similar variations in the AW transport; a switch between maximal and sub-maximal exchange is also

possible. Such switching has been proposed by Garrett et al. (1990a, b), who put forward the existence of an annual cycle linked to the winter formation of Mediterranean deep water. The cycle assigns maximal exchange during the first 6 months, peaking in March, and submaximal during the second half of the year. These authors do not, however, disregard switching of shorter periods, mainly due to barotropic fluctuations of the transport induced by atmospheric forcing. How these fluctuations affect the surface cross-slope (or $\Delta\zeta$) depends on the state of the exchange. Bormans and Garrett (1989b) have studied this subject. Independently of the state of the exchange, an increase of Δp_a (according to the criterion in Fig. 9B) is followed by an increase of $\Delta\zeta$. For a given Δp_a, their model predicts slightly larger variations of $\Delta\zeta$ for sub-maximal exchange but the total $\Delta\zeta$ (mean plus fluctuating part) is always greater for maximal exchange. Table 2 summarizes the prediction of their model for several selected events specified in column 1. In general terms, the observed variations (column 6) are in reasonable agreement with those predicted, but these values do not allow us to discriminate the state of the exchange due to the small differences between columns 4 and 5. However, the $\Delta\zeta$ drop from 10 to 16 July largely exceeds the values predicted by the model. If we admit that the exchange was maximal on 10 July and changed to sub-maximal some time before 16 July, then a large drop of $\Delta\zeta$ (about 11 cm) is also predicted by the model as well as a consistent decrease of U (somewhat larger than the value in Table 2; Bormans and Garrett, 1989a). And this can take place without appreciable change of the inflowing mass transport (i.e. Candela's prediction) since now the layer of AW is considerably thicker. This event could be an example of the mentioned switching. The possibility of a subsequent recovery of maximal exchange (and a further decay to sub-maximal) around 20 July could not be disregarded. Thus, it is not unreasonable to assume that velocity variations are caused by changes in the state of the water exchange. According to

Table 2
Variations of $\Delta\varsigma$ and ΔU induced by variations of Δp_a (column 2)

Event	Δp_a (mb)	Q_b (Sv)	$\Delta(\Delta\varsigma)_{SP}$ (cm)	$\Delta(\Delta\varsigma)_{SB}$ (cm)	$\Delta(\Delta\varsigma)_{OBS}$ (cm)	ΔU (cm s^{-1})
$3 \rightarrow 6$ (1)	+ 5.00	+ 0.40	+ 2.1	+ 3.1	+ 3.9	+ 24.8
$6 \rightarrow 8$ (2)	− 4.50	− 0.36	− 1.8	− 2.6	− 3.1	− 19.7
$8 \rightarrow 10$ (3)	+ 9.00	+ 0.72	+ 3.6	+ 5.1	+ 3.2	+ 20.4
$10 \rightarrow 16$ (4)	− 6.00	− 0.48	− 2.4	− 3.3	− 7.6	− 48.4
$16 \rightarrow 19$ (5)	+ 4.25	+ 0.34	+ 1.8	+ 2.4	+ 3.3	+ 21.0
$19 \rightarrow 23$ (6)	− 9.00	− 0.72	− 3.8	− 5.5	− 4.7	− 29.9

First column indicates the dates between which Δp_a is calculated from data in Fig. 9(B); numbers inside brackets help identify the selected events as shown in this figure. Column 3 represents the induced barotropic transport evaluated from Candela's model with a gain of 0.08 Sv mb^{-1}. Column 4 is the associated variation of $\Delta\varsigma$ estimated from Borman and Garrett's model using the values of column 3 as input in case of maximal exchange. Column 5 is like column 4 but for sub-maximal exchange. Column 6 is the observed variation of $\Delta\varsigma$ from data of Fig. 9(A). The last column represents the values of ΔU deduced from Eq. (4).

the annual cycle suggested by Garrett et al. (1990b), July would be a transition month from maximal to sub-maximal exchange. Then, minor causes may have dramatic effects, that is, relatively small changes in atmospheric pressure can trigger the change.

5. Conclusions

From observations taken during the ICTIOALBORAN-93 survey we have described some atypical features that can be a consequence of the variability of the surface circulation in the Western Basin of the Alboran Sea. One of them was a north to south transport of MSW across the Atlantic Jet. The invoked mechanism is an eddy shedding from the Jet in the neighbourhood of Cape Tres Forcas, where the flow is forced to describe a pronounced meander. We have related the process to the inflow variability through the Strait of Gibraltar driven by atmospheric forcing and, perhaps, by changes in the hydraulic state of the baroclinic exchange through it.

To illustrate our point of view of the whole process we have elaborated the cartoon of Fig. 10, which summarizes the results discussed in previous sections. The sequence is as follows: (A) the AW went out of the Strait at high speed (large sea level difference, supercritical flow?) and after a short way around the WG arrived at the Eastern Basin. It spent little time in the Western Basin so it still kept its Atlantic salinity ($\simeq 36.5$) after crossing it. Probably, the low salinity AW found in the core of the EG arrived there by the date of image 7a. (B) The inflow speed decreased noticeably (subcritical flow?), favouring the growth of the WG. (C) Colder and faster waters have begun to come in the Alboran Sea (supercritical flow recovery?). It could not go around the WG (high Coriolis force vs relatively weak pressure gradient) and burst directly into the existing WG, which was shifted to the east and stretched. It could be that a new gyre is being generated just east of the Strait. The shadowed area represents the MSW that finally will form the core of the cyclonic eddy. (D) The inflow decreased its speed (new change to sub-critical?) allowing the growth of the new gyre in the same way as in (B). A second and more probable evolution is a merging of new and old gyres. In any case, the AW water that had been entering the Alboran Sea since, more or less, the date of diagram C would have been trapped in the Western Basin and the water leaving it would have been an older and saltier AW. Curvature of the eastward vein of the Jet near Cape Tres Forcas was very pronounced. The subsequent likely evolution is represented on diagram (E): cyclonic eddy observed by field sampling on 25 July has been shed from the Jet due to the increased curvature (there are no available satellite images on these days to check this point). Saltier AW would have gone upon entering the Eastern Basin. (F) A "usual" situation was found again. The cyclonic eddy would have lost its identity because of its small size.

We have speculated about the possibility that the evolution in the Alboran Sea during July had been the result of changes in the state of the exchange through the Strait of a few days of periodicity, driven by atmospheric pressure variations. While an

attractive hypothesis, the question remains open for future studies. *In situ* measurements of the properties of the inflow in the eastern section of the Strait of Gibraltar together with flow measurements in the passage between Alboran Island and Cape Tres Forcas would shed light on the problem of stability and evolution of the Alboran Gyres.

Acknowledgements

References

Armi, L., Farmer, D.M., 1988. The flow of Atlantic water through the Strait of Gibraltar. Progress in Oceanography 22, 1–106.

Bormans, M., Garrett, C., 1989a. The effect of rotation on the surface inflow through the Strait of Gibraltar. Journal of Physical Oceanography 19, 1535–1542.

Bormans, M., Garrett, C., 1989b. The effects of nonrectangular cross section, friction and barotropic fluctuations on the exchange through the Strait of Gibraltar. Journal of Physical Oceanography 19, 1543–1557.

Bryden, H.L., Kinder, T.H., 1991. Steady two-layer exchange through the Strait of Gibraltar. Deep-Sea Research 38, S445–S463.

Candela, J., Winant, C.D., Bryden, H.L., 1989. Meteorologically forced subinertial flows through the Strait of Gibraltar. Journal of Geophysical Research 94, 12667–12674.

Cano, N., 1977. Resultados de la campaña "Alboran 73". Boletín del Instituto Español de Oceanografia 1, 103–176.

Donde va Group, 1984. Donde va? An oceanographic experiment in the Alboran Sea. EOS Transactions of American Geophysical Union 65, 682–683.

Donguy, J.R., 1962. Hydrologie en mar d'Alboran. Cahiers Oceanographiques 14, 573–578.

Garrett, C., Akerley, J., Thompson, K., 1989. Low-frequency fluctuations in the Strait of Gibraltar from MEDALPEX sea level data. Journal of Physical Oceanography 19, 1682–1696.

Garrett, C., Bormans, M., Thompson, K., 1990a. Is the exchange through the Strait of Gibraltar maximal or submaximal? In *The Physical Oceanography of the Sea Straits*, L.J. Pratt, editor, pp. 271–294. Kluwer, Boston.

Garrett, C., Thompson, K., Blanchard, W., 1990b. Sea level flips. Nature 348, 292.

Gleizon, P., 1994. Etude experimentale de la formation et de la estabilite de tourbillons anticicloniques engendres par un courant barocline issu d'un detroit. Application a la mer d'Alboran. These de Doctorat de l'Universite Joseph Fourier-Grenoble I.

Groves, G.W., 1955. Numerical filters for discrimination against tidal periodicities. Transactions of American Geophysical Union 36, 1073–1084.

Heburn, G.W., La Violette, P.E., 1990. Variations in the structure of the anticyclonic gyres found in the Alboran sea. Journal of Geophysical Research 95, 1599–1613.

Kinder, T.H., Bryden, H.L., 1987. The 1985–1986 Gibraltar experiment: data collection and numerical results. EOS Transcaction of American Geophysical Union 68, 786–795.

Lanoix, F., 1974. Projet Alboran. Etude hydrologique et dynamique de la Mer d'Alboran. Raport Technique OTAN No. 66.

La Violette, P.E., 1984. The advection of mesoscale thermal features in the Alboran Sea gyre. Journal of Physical Oceanography 14, 550–565.

La Violette, P.E., 1990. The western Mediterranean circulation experiment (WMCE): introduction. Journal of Geophysical Research 95, 1511–1514.

La Violette, P.E., Holyer, R.J., 1988. Noise and temperature gradients in multichannel sea surface temperature imagery of the ocean. Remote Sensing of Environment 25, 231–241.

Lobel, P.S.K., Robinson, A.R., 1986. Transport and entrapment of fish larvae by ocean mesoscale eddies and currents in Hawaiian waters. Deep-Sea Research 33, 483–500.

Millero, F.J., Poisson, A., 1981. International one-atmosphere equation of state of sea water. Deep-Sea Research 28, 625–629.

Mullineaux, L.S., 1993. Implications of mesoscale flows for dispersal of deep-sea larvae. Woods Hole Oceanographic Institution Technical Report No. 7956.

Parrilla, G., 1984. Situación del giro anticiclónico en el mar de Alboran en abril de 1980. Boletín del Instituto Español de Ocanografía 1, 106–113.

Perkins, H., Kinder, T., La Violette, P., 1990. The atlantic inflow in the western Alboran Sea. Journal of Physical Oceanography 20, 242–263.

Preller, R.H., 1986. A numerical model study of the Alboran Sea gyre. Progress in Oceanography 16, 113–146.

Rubín, J.P., Gil, J., Rodriguez, V., Blanco, J.M., Echevarria, F., Rodriguez, J., Jimenez, F., Bautista, B., 1994. Relaciones entre distribución ictioplanctónica, hidrología, biomasa y pigmentos fitoplanctónicos, oxígeno disuelto y nutrientes en el mar de Alborán (Julio 1992). Informes Técnico del Instituto Español de Oceanografía No. 146.

Rubín, J.P., Cano, N., Rodriguez, V., Blanco, J.M., Jimenez, F., Rodriguez, J., Garcia Lafuente, J., Echevarria, F., Guerrero, F.J., Escanez, J., Hernandez, A., Chbani, M., 1997. Relaciones del ictioplancton con la hidrologia, biomasa fitoplanctónica, oxigeno disuelto y nutrientes en el Mar de Alborán y Estrecho de Gibraltar (Julio de 1993). Publiaciones Especiales del Instituto Espagñol de Oceanografia 24, 75–84.

Sambuco, E., Whitehead, J.A., 1976. Hydraulic control by a wide weir in a rotating fluid. Journal of Fluid Mechanics 73, 521–528.

Seco, E., 1959. La capa de velocidad cero en el mar de Alboran. Revista de las Ciencias 25, 765–779.

Speich, S., 1992. Etude du forçage de la circulation oceanique par le detroits: Cas de la Mer d'Alboran. These de Doctoral de l'Universite de Paris VI.

Tintore, J., Gomis, D., Alonso, S., Parrilla, G., 1991. Vertical dynamics and vertical motions in the Alboran Sea. Journal of Physical Oceanography 21, 811–823.

Villalobos, J.A., Villanueva, P., Ruiz, A., 1989. Manifestación de un afloramiento en el sector Se del Mar de Alboran. Scientia Marina 53, 59–65.

Viudez, A., Tintore, J., Haney, R.L., 1996. Circulation in the Alboran Sea as determined by quasi-synoptic hydrographic observations. Part 1. Three-dimensional structures of the two anticyclonic gyres. Journal of Physical Oceanography 26, 684–705.

Werner, A.J., Cantos-Figuerola, A., Parrilla, G., 1988. A sensitivity study of reduced channel flows with application to the Alboran Sea. Journal of Physical Oceanography 18, 373–383.

Whitehead, J.A., 1985. The deflection of a baroclinic jet by a wall in a rotating fluid. Journal of Fluid Mechanics 157, 79–93.

Whitehead, J.A., Miller, A.R., 1979. Laboratory simulation of the gyre in the Alboran Sea. Journal of Geophysical Research 84, 3733–3742.